XL CILAMCE
IBERO-LATIN AMERICAN CONGRESS ON COMPUTATIONAL METHODS IN ENGINEERING
NOVEMBER 11-14, 2019
Praiamar Natal Hotel & Convention
Natal, RN-BRAZIL

# DYNAMIC ANALYSIS OF ONSHORE WIND TURBINES FROM A LAGRAGEAN APPROACH

**Henrique A. N. Castro Filho**
**Suzana M. Ávila**
*Hcastro3009@gmail.com*
*suzana.avila@gmail.com*
*UnB - Gama-DF*
*Brasília Df , Brazil*
**José L. V. de Brito**
*jlbrito@unb.br*
*UnB – Faculdade de Tecnologia*
*Brasília Df , Brazil*

**Abstract.** Special structures, such as wind turbines, have characteristics and exhibit significantly different behavior than conventional civil engineering structures. Wind turbines are generally flexible structures and susceptible to considerable displacement due to external vibrations. Thus, it is of significant importance to analyze the dynamic behavior of these structures. Considering this, the present study aims to evaluate the dynamic performance of wind turbines through two approximate models, investigating three different conditions and how each one will affect the results. The three studied aspects are the influence of the operational condition (parked and rotating), the influence of SSI and the influence of rotor speed. The NREL 5MW wind turbine will be the source of tower, nacelle and rotor properties. The models use multi-degrees of freedom to represent an onshore wind turbine of horizontal axes; in addition, the Euler-Lagrangian approach is used to process dynamic analysis. The first model was developed using rotary blades modeled as continuous beams. The whole model has 8 degrees of freedom. The blades are analyzed as a system of two degrees of freedom, that is, it is possible to vibrate in the directions in the plane and out of the plane. They are connected in the center of the tower-nacelle represented by a spring of mass corresponding to a system of two degrees of freedom, that is to say, also can have vibrations in the directions in the plane and outside the plane. The second model has the same characteristics as the first; however, a foundation shaped like a spring with bi-directional rotational stiffness is included therein. In this way, it is possible, from this model, to study the soil-structure interaction (SSI). Soil stiffness and damping properties were acquired from the DNV/Risø standards and are used as a comparison. A wind load and an earthquake are used as a source of vibration for the models. The main objective, then, is to evaluate the impact of three different conditions through the dynamic response obtained from the two models. From the results, it can be seen that the responses of the wind turbine in the operating condition are much larger than those in the parked condition; SSI can greatly affect tower responses; however, does not have a significant effect on the vibrations occurring in the plane of rotation of the blades. Finally, it is realized that the amplitude of the response increases with the velocity of the rotor, in general.

**Keywords:** Onshore Wind Turbine; Operating Condition; SSI; Velocity of the Rotor.

# 1 Introduction

Wind turbines play an important role in the production of electricity. Certainly, like any energy production system, the idea is to extract energy from the winds in the most efficient way possible. To optimize, the process of power generation, wind turbines have adopted in the current projects, slender towers, and large rotors. This project profile implies wind turbines more vulnerable to vibration. Common excitation sources in wind turbines are, for example, wind loads, sea waves (offshore wind turbines), which are constantly experienced throughout the life of a wind turbine, or even exceptional actions such as earthquakes [1]. The problems arising from external vibrations are diverse, they can, for example, compromise the production of wind energy, cause fatigue damage to structural components and even the collapse of the structure. Therefore, in order to ensure the safe and efficient operation of wind turbines, it is essential to accurately understand the dynamic behavior of these structures during their lifetime [2]. The notability of this field of study can be perceived by the interest in this area in the recent years. Several researches have been conducted by different scholars to investigate the dynamic behavior of wind turbines under the action of wind, sea waves and / or seismic loads [3]. A very relevant work for this area of study was developed by Prowell et al. [4]. To investigate the influence of operational condition on the dynamic behavior of wind turbines, the researchers performed tests on a vibration table. Thus, they investigated the seismic responses and concluded that additional damping in the out-of-plane direction of vibration was observed compared to the parked condition. The work of Prowell et al. used real-scale turbines to perform the experiments.

In addition to experimental tests, there are several studies that use analytical models to obtain the dynamic responses of aerogenerators. Harte et al. [2] and Fitzgerald et al. [5], for example, use analytical models, in which they simplified each blade as a system of a single degree of freedom, Fitzgerald & Basu [6] considered two degrees of freedom to represent each blade and two degrees to represent the tower. In these two studies, the Lagrangian approach was used to solve the equations of motion and the dynamic responses were estimated using MATLAB. It is concluded that the responses of the wind turbine in the operating condition are much higher than those in the parked condition. It is also verified that the soil-structure interaction can significantly affect the displacement of the tower; however, does not have a significant effect on the vibrations occurring in the plane of rotation of the blades.

Another aspect of wind turbines that have been well studied is the influence of soil-structure interaction (SSI) on these structures. In a pioneering study in 1973, Veletsos and Verbic [7] showed that the presence of flexible soil under the foundation of a structure increases the damping capacity of the foundation and reduces the natural frequency of the structure. The same was also observed in a report by Stewart et al. [8]. They concluded that the SSI generally has the effect of lengthening the periods of vibration of the structures, which can be cause for concern because the location of the wind-induced spectral energy is at low frequencies.

The SSI study for wind turbine structures has progressed considerably from the work of Lombardi et al. [9] and Bhattacharya and Adhikari [10]. They performed models from analytical methods incorporating the rotational and translational flexibility of the foundation. New experimental techniques were developed to obtain the necessary parameters for the analytical model. In this work, the analytical model was validated using a finite element approach and compared with experimental measurements. The results show that the natural frequencies and damping factors of the wind turbine change significantly with the soil/foundation type.

In other relevant work, Austin and Jerath [11] analyzed the effects of soil-foundation-structure interaction on the seismic response of 65 kW, 1 MW and 2 MW horizontal axis wind turbines with steel towers. Four types of foundations were analyzed, including foundations such as shoe, mono-pile, pile group and anchored foundation. The soil is implicitly modeled (subgrade reaction module) and explicitly. It was concluded that fort the specific cases studied, the effect of soil-structure interaction on the seismic response of wind turbines is significant mainly for shallow foundations such as shoes. Therefore, the seismic analysis of wind turbine towers in these cases should be considered. Following

this line of research on the study of dynamic effects of wind turbines, this work seeks to contribute with some aspects considered relevant. First, this article brings together three analyzes of important aspects in the study of the behavior of aerogenerators, aspects that can be found in separate articles, but rarely in the same study. These aspects are the influence of the operational condition (parked and rotating turbine), the influence of SSI and the influence of rotor speed. Additionally, another relevant aspect in this study is the use of an earthquake and a wind spectrum as a source of external vibration, something that is difficult to find in studies that use analytical models with the Lagrangian approach. Finally, another contribution of this study is the developed analytical model, which, because of its good detail and simplified understanding, can be used to study the responses of other types of wind turbines, since in this article the adopted turbine is the NREL 5MW.

In order to study the dynamic behavior of wind turbines, two models were developed in this work. These models were adapted from the works developed by Harte et al. [2] and Fitzgerald & Basu [6]. The first model initially presents eight degrees of freedom, consisting of three blades (two degrees of freedom for each blade) and a tower + nacelle represented by a concentrated mass with two degrees of freedom. From the eight degrees of freedom model described above, two degrees of freedom were added in order to study the SSI, thus completing the second model. The properties of the model were extracted from the real NREL 5MW turbine [12]. The soil-structure interaction model presents two degrees of freedom that are dependent on the damping, stiffness and mass of the soil adopted. Three soils were considered in this study to verify the influence of SSI, and these are analyzed using the DNV / Risø design practice [13].

## 2 Model

In order to define the analytical model to be studied, several studies were taken into account. The work of: Murtagh et al. [14] Harte et al. [2], Staino & Basu [15], Fitzgerald et al. [5], Fitzgerald & Basu [6], Zhang et al. [16], Zuo et al. [1]. To adapt a model from these already presented in the literature, some parameters of choice were defined, being these: model that did not demand great computational cost, known mathematical approach, parameters to be able to study the interaction soil-structure, possibility of studying the movement of the blades and tower in the two main directions, and the possibility of studying the influence of the speed of rotation of the blades. Thus, analyzing all these requirements, the wind turbine model chosen to be studied in this dissertation was adapted mainly from the works of Fitzgerald & Basu [6] and Harte et al. [2].

Thus, two models were adapted to investigate the objectives proposed for this study; based on work [6] and [2]. The first model (Figure 1) was developed using rotary blades modeled as continuous beams. The whole model has 8 degrees of freedom. The blades are analyzed as a system of two degrees of freedom, that is, the vibrations are considered in the in-plane and out-of-plane directions. They are connected in the center to the tower + nacelle represented by a mass + spring system corresponding to a system of two degrees of freedom, that is, it can also have vibrations in-plane and out-of-plane Figure 1.

The second model has the same characteristics of model 1, however it is included in it a foundation modeled as a spring with bi-directional rotational stiffness (Figure 2). Thus, it is possible, from this model, to study the SSI, as can be seen in the Figure 2. With the two degrees of freedom added to model 1, the second model has a total of 10 degree of freedom.

In this article we consider the following notation: the subscript *'i'* refers to the paddles (i = 1, 2 and 3), the subscript *'n'* refers to the tower, and the *'in'* and *'out'* subscripts refer to in-plane and out-of-plane movements, respectively.

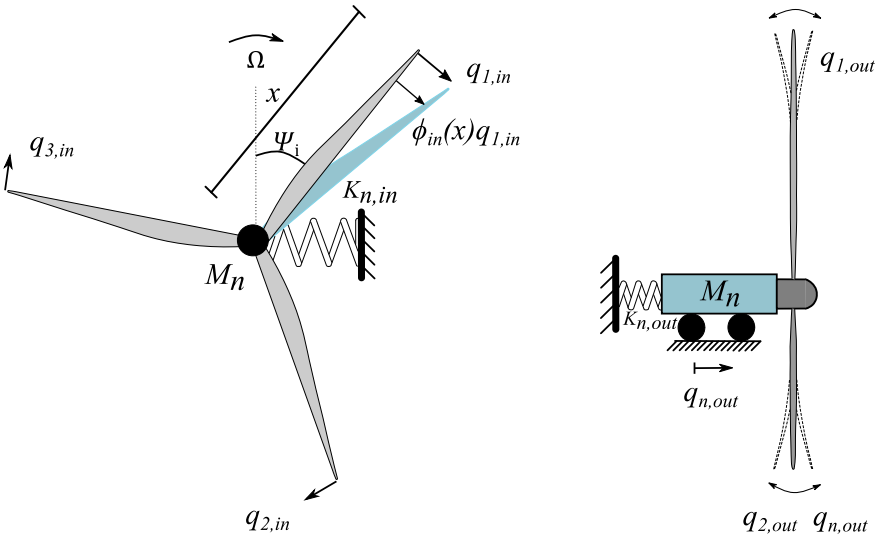


In-plane vibration Out-of-plane vibration

Figure 1: Model with 8 degrees of freedom and clamped foundation. Source: Fitzgerald & Basu [6] adapted.

The model consists, as previously mentioned, of three blades treated as rotating beams of length L, with flexural stiffness *EI(x)* and mass $(\mu(x))$ along the length. The blades rotate at a constant speed $(\Omega)$ about the rotor axis, i.e., the rotational speed does not vary with time. The azimuthal angle of the blade *'i'* at the instant of time 't' is given by Equation (1). The azimuth $\Psi_i$ corresponds to the blade in the vertical position.

$$\Psi_i = \Omega\, t + \frac{2\pi}{3}(i-1) \tag{1}$$

As can be seen in Figure 1 and Figure 2, the degrees of freedom corresponding to the in-plane and out-of-plane vibrations are defined by $q_{i,in}(t)$ and $q_{i,out}(t)$. The in-plane ($\phi_{in(x)}$) and out-of-plane ($\phi$out(x)) vibration modes must be normalized so that $q_{i,in}(t)$ and $q_{i,out}(t)$ represent the displacements at the tip of the blade, in the in-plane and out-of-plane directions, respectively.

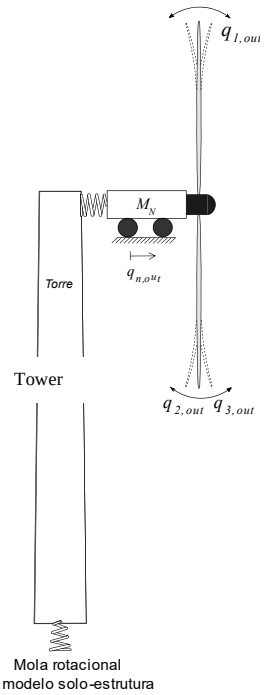


Figure 2: Wind turbine model considering the SSI. Source: Fitzgerald & Basu [6] adapted.



Rotational spring - SSI

It is assumed that the out-of-plane and out-of-plane displacements at any point at a distance x from the hub-hub hub are represented by $u_{i,in}$ (x,t) and $u_{i,out}$ (x,t), calculated in terms of the fundamental vibration modes of the blades, as shown in Equations (2) and (3).

$$u_{i,in}(x,t) = \phi_{in}(x) q_{i,in}(t) \tag{2}$$

$$u_{i,\text{out}}(x,t) = \phi_{out}(x) q_{i,\text{out}}(t) \tag{3}$$

From Equations (2) and (3), it is shown that the development of the analytical model is dependent on the function of the vibration mode of the blade. According to Clough & Penzien [18], to obtain an equation that represents the mode of vibration of the blade, proceed as follows: model the blade using software in finite elements; perform a modal analysis; obtaining the displacement values for the first vibration mode; and finally, to approximate the results to a polynomial function and this will describe the vibration modes of the blades, $\phi_{in}(\bar{x})$ and $\phi_{out}(\bar{x})$ . Thus, proceeding as specified above are Equations (4) and (5).

$$\phi_{in}(\bar{x}) = -0,6893 \cdot \bar{x}^6 + 2,3738 \cdot \bar{x}^5 - 3,6043 \cdot \bar{x}^4 + 2,5737 \cdot \bar{x}^3 + 0,3461 \cdot \bar{x}^2 \tag{4}$$

$$\phi_{out}(\bar{x}) = -2,4766 \cdot \bar{x}^6 + 5,1976 \cdot \bar{x}^5 - 3,4820 \cdot \bar{x}^4 + 1,7085 \cdot \bar{x}^3 + 0,0525 \cdot \bar{x}^2 \tag{5}$$

Wherein:

$\bar{x} = x / L$

$L = blade\ length.$

Figure 3 illustrates the modals shape $\phi_{in}(\bar{x})$ and $\phi_{in}(\bar{x})$ for the blades used in this work. Note that because of greater inertia in the off-plane direction, the deformation is closer to a straight line, ie, the curve of the function is less steep.

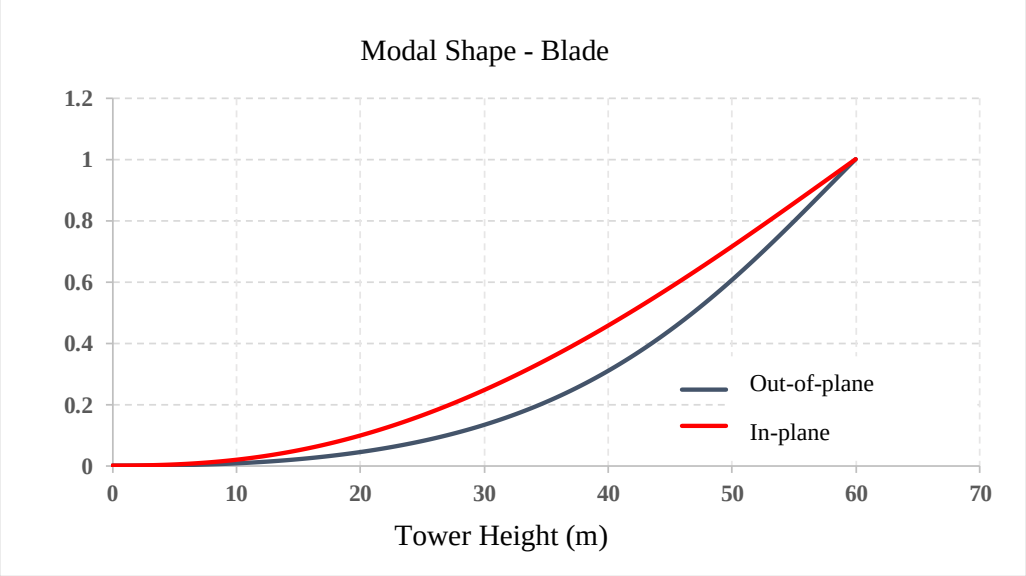


Figure 3: Function of the first blade vibration mode in both directions.

For the model, besides the displacement, it is interesting to know also the angle variation from the displacement. According to Clough and Penzien (2013), this variation can be expressed by Equations (6) and (7).

$$\theta_{i,in} = \frac{\partial u_{i,in}}{\partial x} \tag{6}$$

$$\theta_{i,\text{out}} = \frac{\partial u_{i,\text{out}}}{\partial x} \tag{7}$$

## 2.1 Properties

The model properties for blades, nacelle and tower were defined from the characteristics of a 5 MW NREL wind turbine with 3 blades and are presented in Table 1 e Table 1 [1].

Table 1: Properties of the model. Source: Zuo *et al*. (2018).

| **NREL 5MW - Properties** | | |
|---|---|---|
| **General description** | Maximum rated power | 5MW |
| | Rotor orientation | Upwind, 3 pás |
| **Blade** | Diameter of the rotor | 126 m |
| | Height of the Hub | 90 m |
| | Velocity (rotor): *cut-in, nominal e cut-out* | 6,9 rpm; 12,1 rpm e 20 rpm |
| | Length | 61,5 m |
| | Total mass (integrated) | 17740 kg |
| **Hub and Nacelle** | Diameter*(hub)* | 3 m |
| | Mass *(hub)* | 56.780 kg |
| | Mass *(nacelle)* | 240.000 kg |
| **Tower** | Height | 87,6 m |
| | Mass | 347.460 kg |
| | Structural damping | 1% |

Table 2: Material properties. Source: Zuo *et al*. (2018).

| **Component** | **Material** | **Density (kg/m³)** | **Young's modulus (GPa)** | **Poisson** |
|---|---|---|---|---|
| **Blade** | Polyester | 1850 | 38 | 0,3 |
| **Tower** | Steel | 8500 | 210 | 0,3 |

## 2.2 Mathematical Formulation

The equations of motion of the system can be obtained from the Lagrange equation (Eq. (8)(8)).

$$\frac{\partial T}{\partial \dot{q}_i} - \frac{\partial T}{\partial q_i} + \frac{\partial V}{\partial q_i} = \mathrm{Q}_i \tag{8}$$

The Eq. (8) depends on potential (*V*) and kinetic energy (*T*). Thus, to define the equation of motion of the systems through the Euler-Lagrange equation, it is first necessary to define the equations of potential and kinetic energies.

- **Total Potential Energy**

For the analysis of potential energy, the criterion adopted was based on Hansen [20]. In this work, the author states that the total potential energy of the system (*V*) must be obtained considering the potential energy of the blade in the flexion, the contribution of the centrifugal force, the contribution from the gravity component along the axis of the blade and the potential energy of the nacelle. In this way, these will be the energy equations deduced below.

*Potential energy of the blade in bending*

For the model studied, the portion of potential energy from the blade flexion can be calculated as half the sum of the moments multiplied by the respective angles of the deformed, as shown in Eq. (9) [18].

$$\frac{1}{2}\cdot\int_0^L\left(EI(x)\frac{\partial\theta_i}{\partial x}\right)\frac{\partial\theta_i}{\partial x}dx\rightarrow\frac{1}{2}\cdot\int_0^L EI(x)\left(\frac{\partial\theta_i}{\partial x}\right)^2dx \tag{9}$$

*Potential energy due to the contribution of centrifugal force*

Another part of the system's energy comes from the rotation of the blades, as this rotating movement contributes to the stiffness and consequently adds energy to the system. The rotation generates in the blades a tensile force *N(x)* so that this force adds to the system an increase in potential energy. *N (x)* can be calculated as a function of the rotor speed ($\Omega$) and mass ($\mu(x)\cdot x$) as shown in Eq. (10)(10).

$$N(x)=\Omega^2\int_x^L\left(\mu(\mathrm{x})\cdot x\right)d\xi \tag{10}$$

Knowing the Force *N(x)*, and knowing that the force that performs work is equal to $F=N(x)\cdot\theta$, it can be calculated the energy as half of the sum of the product of the force *F* by the displacement as follows:

$$\begin{aligned}U=\frac{1}{2}F\cdot u\rightarrow dU&=\frac{1}{2}\int_0^L\left(N(x)\cdot\theta\right)\partial u\left(\frac{dx}{dx}\right)\\ Energy\ (\text{rotation of the blades})&=\frac{1}{2}\int_0^L\left(N(x)\right)\left(\frac{\partial u}{\partial x}\right)^2dx\end{aligned} \tag{11}$$

*Energy due to gravity acting on blades*

As a wind turbine blade system is rotating, the force of gravity acting on the blades is variable with time. Thus, the effect from gravity is modified for each position of the blade. At the bottom of the rotating circle, for example, gravity is generating a pull on the blades, just the opposite happens when the blades are at the top; in this position the weight itself is compressing them. In this way, the energy coming from the action of the blade weight varies according to the position angle.

The gravitational force (*G(x)*) can be obtained by the Eq. (12).

$$G(x)=-\frac{1}{2}g\cdot\cos\left(\Psi_i\right)\int_x^L\left(\mu(\mathrm{x})\right)dx \tag{12}$$

Wherein ($\Psi_i$) is the angle that defines the position of the blade.

As previously defined, the azimuth $0^\circ$ corresponds to the blade in the vertical position. The term of the equation that defines whether gravity is pulling, compressing or flipping the blades is the position angle $\Psi_i$. It can be calculated by Eq. (1).

Knowing the force *G*(x), and knowing that the force that performs work is equal to $F=G(x)\cdot\theta$, it is possible to calculate the energy from Eq. (13).

$$Energy\ \left(gravity\ acting\ on\ the\ blades\right)=\int_0^L\mathrm{G}(x)\left(\frac{\partial u_i}{\partial x}\right)^2dx \tag{13}$$

*Energy Potential Elastic - (Nacelle + Tower)*

In the model studied, the only component modeled as a mass-spring system is the tower + nacelle. In this way, the elastic potential energy can be extracted directly by the Eq. (14).

$$Energia\ potencial\ elástica = \frac{1}{2} k_n q_n^2 \tag{14}$$

*Lagrangian: Total Potential Energy*

After analyzing each term of the potential energy, it is possible to formulate the Lagrangian that defines the total potential energy. For each of the four parts of the potential energy described, it is necessary to consider the components in the plane and out-of-plane. By doing so, we find the total potential energy of the system (Eq. (15)).

$$\begin{aligned} V = \frac{1}{2}\sum_{i=1}^{3}\int_0^L & \left[ EI_{in}(x)\left(\frac{\partial \theta_{i,in}}{\partial x}\right)^2 dx + EI_{out}(x)\left(\frac{\partial \theta_{i,\text{out}}}{\partial x}\right)^2 dx + 2EI_{inout}(x)\left(\frac{\partial \theta_{i,in}}{\partial x}\right)\left(\frac{\partial \theta_{i,\text{out}}}{\partial x}\right) dx \right. \\ & \left. + N(x)\left(\frac{\partial u_{i,in}}{\partial x}\right)^2 dx + N(x)\left(\frac{\partial u_{i,\text{out}}}{\partial x}\right)^2 dx + G(x)\left(\frac{\partial u_{i,in}}{\partial x}\right)^2 dx + G(x)\left(\frac{\partial u_{i,\text{out}}}{\partial x}\right)^2 dx \right] \\ & + \frac{1}{2} k_{n,in} q_{n,in}^2 + \frac{1}{2} k_{n,\text{out}} q_{n,\text{out}}^2 \end{aligned} \tag{15}$$

- **Total Kinetic Energy**

The total kinetic energy of the studied system is divided in the kinetic energy coming from the blades plus the kinetic energy generated by the mass-spring system that represents the tower + nacelle.

*Kinetic energy in the blades*

For the studied system, it is necessary first to define the vector velocity of the blades.

The wind turbine model described in this section considers both blade vibrations in the plane and out of plane, these being coupled. Due to the rotation of the blades, the model was formulated using a position vector with stationary reference point. The position vector, $r_i(t)$, of a given point on the *i*-th blade, at a distance *x* from the center of the hub, has the representation in the rotational coordinate system given by Eq.(16) with the base unit vectors $\vec{i}(\mathrm{t})$, $\vec{j}(\mathrm{t})$ and $\vec{k}(\mathrm{t})$.

$$\begin{aligned} r_i(t) = & \left[ x + q_{n,in} sen(\psi_i) \right] \vec{i}(\mathrm{t}) \\ & + \left[ \phi_{in}(x) \cdot q_{i,in} + q_{n,in} cos(\psi_i) \right] \vec{j}(t) \\ & + \left[ \phi_{out}(x) \cdot q_{i,out} + q_{n,out} \right] \vec{k}(t) \end{aligned} \tag{16}$$

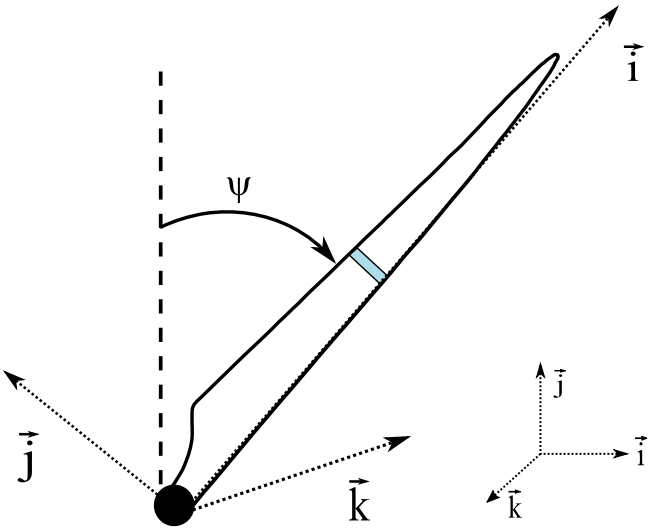


Figure 4: Vector directions.

The vector component $\vec{i}$(t) (x-axis) is composed of the distance *x* plus the displacement of the tower in this direction ($q_{n,in} sen(\psi_i)$). The vector component $\vec{j}$(t) (y-axis) is composed of the deformed blade ($\phi_{in}(x) \cdot q_{i,in}$) plus the displacement of the tower in this direction ($q_{n,in} cos(\psi_i)$). Lastly, the component $\vec{k}$(t) (z axis) will be basically for out-of-plane movements, thus composed of the bent blade ($\phi_{out}(x) \cdot q_{i,out}$) plus the displacement of the tower in this direction ($q_{n,out}$). Thus, from the position vector $r_i(t)$ it can be found the velocity vector $v_i(t)$, since velocity is the derivative of the position by time. Therefore, the velocity vector is expressed in Eq. (17).

$$\begin{aligned} v_i(t) = \dot{r}_i(t) = \\ \left[\dot{q}_{n,in} sen(\psi_i) - \Omega \phi_{in}(x) \cdot q_{i,in}\right] i(\mathrm{t}) \\ + \left[\Omega \cdot x + \phi_{in}(x) \cdot \dot{q}_{n,in} cos(\psi_i)\right] j(t) \\ + \left[\phi_{out}(x) \cdot \dot{q}_{i,out} + \dot{q}_{n,out}\right] k(t) \end{aligned} \tag{17}$$

Once the velocity has been calculated by Eq. (17), it can be can obtained the equation that computes the kinetic energy in the blades (Eq. (18)).

$$T = \frac{1}{2} v_i^2 \int_0^L \mu(x) dx \tag{18}$$

*Kinetic Energy - Tower + nacelle*

Also applying the concept of kinetic energy, it can be calculated the one coming from the mass movement of the tower + nacelle. As it was previously defined that the displacement would be represented by the letter *q* (instead of *x*) and that the subscript n would represent parameters related to nacelle, it is possible to rewrite Eq. (18) in order to obtain Eq. (19).

$$T = \frac{1}{2} M_n \dot{q}_n^2 \tag{19}$$

*Lagrangean: Total Kinetic Energy*

For each of the elements, it is necessary to consider the movements in the plane and out-of-plane. By doing so, we find the total kinetic energy of the system (Eq. (15)).

$$T = \frac{1}{2}\sum_{i=1}^{3}\int_{0}^{L}\mu(x)\upsilon_i^{\,2}dx + \frac{1}{2}M_n\dot{q}_{n,in}^2 + \frac{1}{2}M_n\dot{q}_{n,\text{out}}^2 \tag{20}$$

To find the equation of motion that describes each of the eight degrees of freedom, it is necessary to replace Equations (15) and (20) in Equation (8) and replace the properties of the NREL 5MW turbine.

# 3 Loads

The process of obtaining and applying the loads used in the models presented in this article is described. For this study two external loads are considered, a wind load and a seismic load.

## 3.1 Wind Load

The responses over time of the drag force of the wind are simulated, in this work, according to the classic theory of the Moment of the Spade Element (BEM), that conjugates the theory of the moment with local events that occur in the real blades [21]. BEM is the most popular tool for determining aerodynamic loads on a rotary rotor [20], since satisfactory results can be obtained.

With the BEM method, it is possible to calculate the constant loads of the wind and, therefore, the thrust and power [22]. The wind loads are calculated following an approach given by Hansen [18], which assumes that all sections are independent along the rotor, so that the blade can be divided into several elements and the wind flow in each separately calculated element.

Due to the changes in mean wind speed with height, as the blade rotates the average velocity component in the blades undergoes a sinusoidal variation in magnitude, the frequency of that sine is equal to the rotational frequency of the rotor. Therefore, the instantaneous velocity of the wind can be expressed as:

$$V_i = \bar{\upsilon}(H) + \Delta\upsilon\left(\frac{r}{R}\right)\cos(\Omega\cdot \mathrm{t} + \theta_i) \tag{21}$$

Wherein:

- *H:* is the height of the nacelle;
- $\bar{\upsilon}(H)$: is the average wind speed at the hub height;
- $r$: is the position along the blade; and
- $\Delta\upsilon$: is the change in wind speed between the hub and the top of the blade in the upright position.

The scale factor (*r/R*) is used to calculate the amplitude needed at each point along the blade in order to represent the wind speed varying sine-wave above and below the hub. The term *t* is the time and $\theta_i$ is the phase difference between the blades of the turbines. The relative wind speed, relative to each blade element for each blade, $V_{r,i}(r,t)$ is given by:

$$V_{r,i}(r,t) = \sqrt{\left[V_i(t)\cdot(1-a) + \upsilon^w(t)\right]^2 + \left[\Omega\cdot r\cdot(1+a')\right]^2} \tag{22}$$

Where *a* and *a'* are the axial and tangential induction factors that are calculated by the classical BEM method with corrections. The instantaneous velocity of the apparent wind on the blade, $V_i(t)\cdot(1-a)$, incorporates the average wind speed that varies sine-wave due to wind variation with

blade height and rotation. Turbulence is included only in the normal direction.

The wind load on any structural member can be decomposed into a near-static average velocity of the wind, $V_i$, and a floating turbulent component, $\upsilon^w(t)$. The generation of this floating turbulent component $\upsilon^w(t)$ in the rotor plane is the basis of any aerodynamic simulation and can be obtained through the use of a power spectral density function. Nodal fluctuation velocity profiles varying over time can be simulated by virtue of the fact that an arbitrary velocity profile with zero mean can be represented by a DFT with a discretized version of a continuous frequency content such as:

$$\upsilon^w(t) = \sum_{k=1}^{\infty} a_k \cos(\omega_k t) + \sum_{k=1}^{\infty} b_k sen(\omega_k t) \tag{23}$$

Wherein:

- $a_k$ e $b_k$ : are the Fourier coefficients;
- $\omega_k$ : is the discretized circular frequency; and
- *t*: it is the instant of time.

The floating velocity profile varying with time is generated in conjunction with a wind speed spectrum. Time displacement graphs were simulated using Eq. (24), a modified version of the spectrum offered by Kaimal et al. [23], expressed as:

$$\frac{\mathrm{S}_{\upsilon}(\mathrm{H},\omega)}{\sigma_{\upsilon}^2} = \frac{100c}{3\omega(1+50c)^{5/3}} \tag{24}$$

Wherein:

- $\mathrm{S}_{\upsilon}(\mathrm{H},\omega)$ : is the unilateral spectrum of floating wind speed as a function of hub height and circular frequency ( $\omega$ );
- $\sigma_{\upsilon}^2$ : is the variance (related to the turbulence intensity); and
- *c*: coordinated Monin.

The latter term can be obtained from the expressions:

$$c = \frac{\omega H}{2\pi\bar{\upsilon}(H)} \tag{25}$$

$$\bar{\upsilon}(H) = \frac{1}{k}\upsilon_* \cdot ln\frac{H}{z_0} \tag{26}$$

Wherein:

- *k*: is the Von Karman constant (typically around 0.4);
- $z_0$ : is the roughness length; and
- $\upsilon_*$ : is the rate of friction.

The above formulation was used to generate a homogeneous and isotropic turbulence at the hub height to represent turbulence across the rotor area. Due to the rotation of the blades, the turbulence spectra will be inhomogeneous in nature, leading to a rotation of sampled spectra.

However, the focus of this article is not this study, so the simplified field of turbulence is appropriate. The wind load is taken only in the normal (flap) direction, as only clockwise vibrations are considered. The normal force per unit length of the blade [18] can be expressed as:

$$p_{N,i} = \frac{1}{2}\rho V_{r,i}^2(r,t)\,\mathrm{C}_N(\infty)\,c(r) \tag{27}$$

Wherein

- $\rho$ : is the density of air,
- $c(r)$ : is the radius length,

- $C_N(\infty)$: is the normal coefficient that is dependent on the drag and drag coefficients (which are calculated from tables based on the properties of the blade profile and the angle of attack).

Integrating along the entire length of the rotor blade, the generalized wind load on blade *'i'* can be provided by:

$$F_i(t) = \int_o^R p_{N,i}(x,t)\ \phi_n(x)dx \tag{28}$$

Described the entire process of obtaining the wind load for each model of the model, this value can be entered in the equation of motion as an external force. Replacing all required data in Eq. (28) it is possible, as previously mentioned, with the help of the Matlab software, to solve each EDO and obtain the results of the deformations over time.

### 3.2 Load due to the earthquake - 'El Centro'

Tensions and displacements caused by dynamic excitations can be induced in a structure not only by variable loads, but also by movements of their points of support. Earthquakes are important examples of these types of excitation. The movements of the base generated by the earthquakes cause oscillations in the foundation of the structure due to vibrations of the soil in which it is accommodated.

In this work, as mentioned previously, an excitation from an earthquake was considered as source of external excitation. To introduce the movement generated by the earthquake in the model, it is necessary to express the phenomenon in terms of an equation of motion. Thus, according to Clough and Penzien [18], the equation that introduces the movement of the soil in the structure is described in Equation (29).

$$m\ddot{v}(t) + m\ddot{v}_g(t) + c\dot{v}(t) + kv(t) = 0 \tag{29}$$

Where:

- $\ddot{v}_g$: acceleration of soil; and
- $\ddot{v}$: acceleration caused by the deformation of the structure.

Since the soil acceleration represents the dynamic input specified for the structure, the same equation of motion can be more conveniently written as Eq. (30).

$$m\ddot{v}(t) + c\dot{v}(t) + kv(t) = -m\ddot{v}_g(t) \equiv p_{\text{eff}}(t) \tag{30}$$

In this equation, $p_{\text{eff}}(t)$ denotes the effective excitation load of the carrier; in other words, the structural deformations caused by the soil acceleration ($\ddot{v}_g(\text{t})$) are exactly the same as would be produced by an external load $p(\text{t})$ equal to $-m\ddot{v}_g(\text{t})$.

This same solution method has been expanded to the models studied in this article. As the mass matrix of the system had previously been obtained, only the soil accelerations needed to be defined. The earthquake chosen to be the external source of vibration was the 'El Centro' that occurred in California in 1940; thus, soil accelerations ($\ddot{v}_g(\text{t})$) were obtained from data from this earthquake found in the work of Khosravikia [24]. The seism was inserted in the out-of-plane direction as shown in Figure 5, so only the degrees of freedom corresponding to that direction were excited.

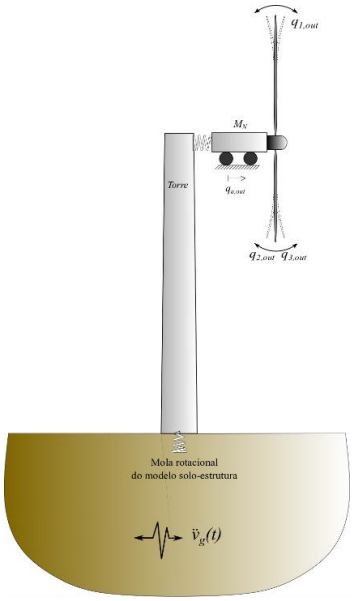


Figure 5: Earthquake inserted in the model.

# 4 SOIL STRUCTURE INTERACTION

Nowadays, in some works, wind turbine foundations have been modeled simply by beam elements or static springs, which means that the stiffness of the foundation is frequency independent [25]. These assumptions are idealized and conservative, so they can potentially lead to an overestimation of rigidity and, therefore, to the natural frequency of the system [26]. Consequently, unless the separation between the operating and natural frequencies is large, these assumptions should not be used and the SSI needs to be considered in the project [27]. Therefore, it is essential to know the overall natural frequency of the structure to allow enough separation of the natural frequency of the structural system from the turbine operating frequencies to avoid potentially catastrophic faults [28]. The soil structure model adopted in this study is composed of a multi degrees of freedom model located on a foundation based on rigid gravity with two degrees of freedom, scaled using the DNV / Risø design practice [13]. Three soils were considered in this study to verify the influence of SSI; their characteristics are described in Table 3.

Table 3: Soil Properties. Source: Lombardi [9].

| | **Es [MPA]** | **$\rho$ [KN/M³]** | $\nu$ |
|---|---|---|---|
| **SOIL 1** | 25 | 16 | 0,35 |
| **SOIL 2** | 50 | 16 | 0,4 |
| **SOIL 3** | 100 | 18 | 0,4 |

# 5 RESULTS

## 5.1 Validation of the model

To validate the model studied here, we used the comparison of the natural frequencies obtained through the model with those found in the literature [17]. For the data of the model studied the results presented in the Table 4.

Table 4: Validation of the model by the natural frequency.

| | **Blade (in-** | **Blade (out-of-** | **Tower (in-** | **Tower (out-of-** |
|---|---|---|---|---|

| | plane) (Hz) | plane) (Hz) | plane) (Hz) | plane) (Hz) |
|---|---|---|---|---|
| **Present study** | 1.114 | 0,641 | 0,301 | 0,303 |
| **Literature [17]** | 1.083 | 0,683 | 0,312 | 0,316 |
| **Difference (%)** | 2,93 | 6,14 | 3,51 | 4,11 |

Analyzing the results of Table 4, it is noticed that the error presented is small and the results are very close. Therefore, the model developed in this work can be considered validated to analyze other situations that are shown in the sequence.

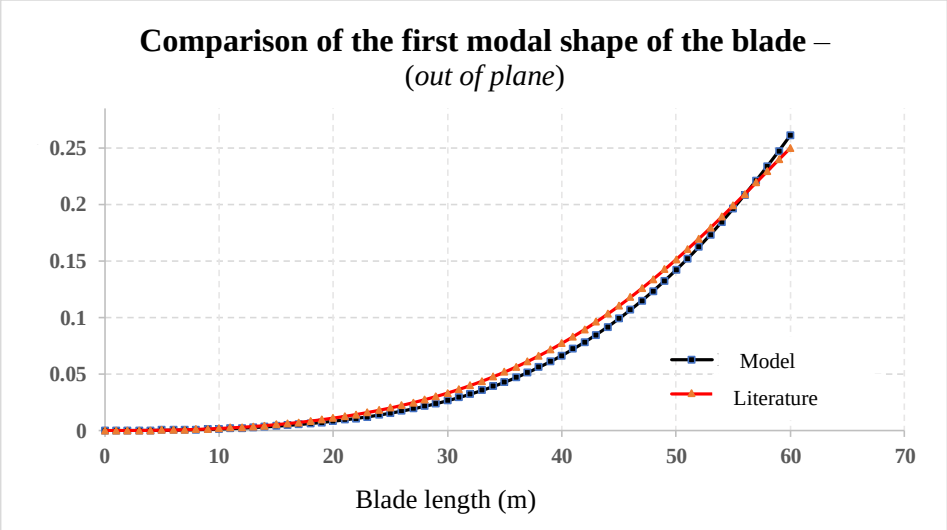


Figure 6 – Comparison of the first modal shape of the blade (out-of-plane).

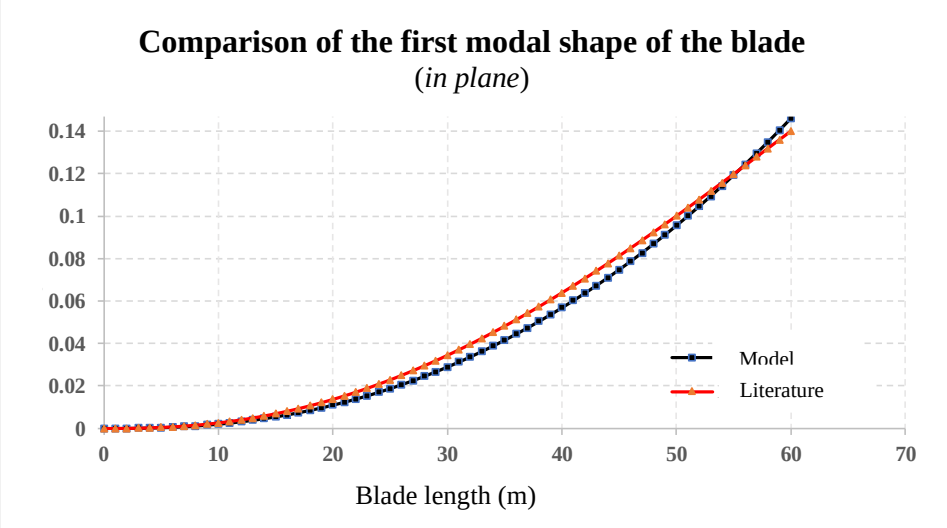


Figure 7 –Comparison of the first modal shape of the blade (in plane).

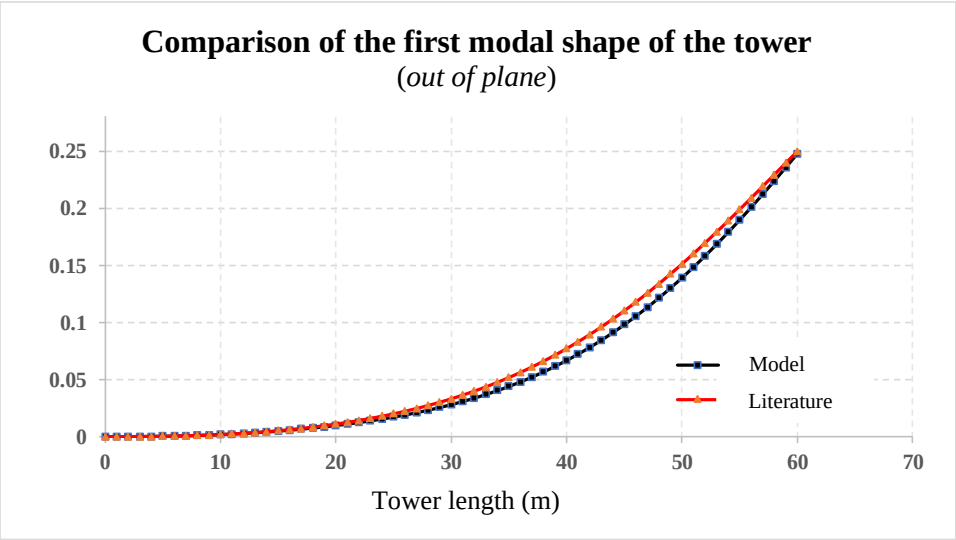


Figure 8 – Comparison of the first modal shape of the blade (out of plane).

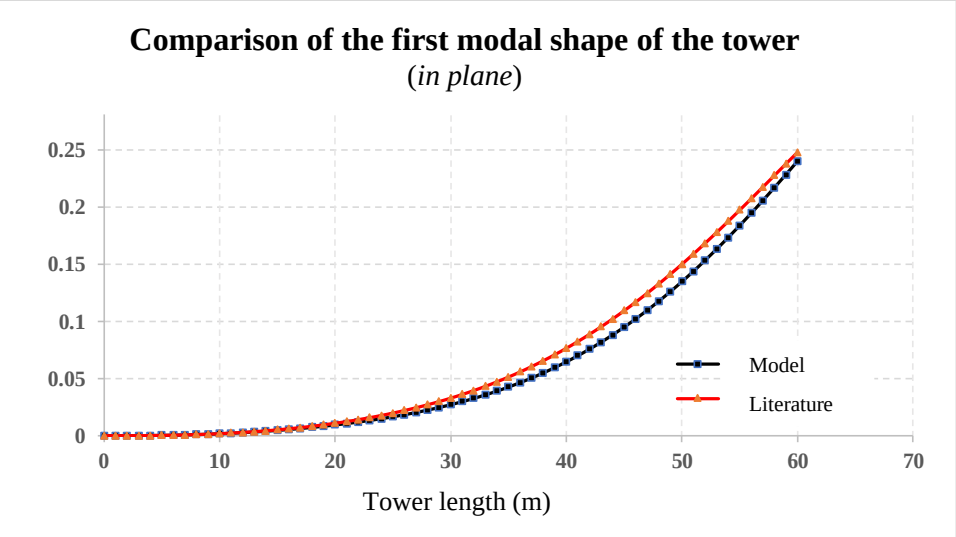


Figure 9 – Comparison of the first modal shape of the blade (in plane plane).

Analyzing the results of Table 4, it can be seen that there is a good agreement between theresults obtained from the and those found in the study by ZUO et al., 2018, in which there are also compared with the literature. As the natural frequency results, the modals shapes of the first mode of vibration shown in Figures 6, 7, 8 and 9 confirm that there is a good agreement between the results obtained with the model used in this study and the NREL 5MW data. Therefore, the model developed in this paper can be considered adequate to analyze other situations shown below.

### 5.2 Influence of operational condition

To examine the influence of wind turbine operating conditions on structural responses, two cases are investigated in this section. In the first case, the wind turbine is in the parked condition, with the position of the blades exactly the same as shown in Figure 1. In the second case, the blades are rotating with a uniform angular velocity of *12.1* rpm, which corresponds to the nominal rotor speed of the NREL 5MW wind turbine. The wind and earthquake loads discussed in section 3 are applied simultaneously to the wind turbine under both conditions. A duration of *50s* is considered for all external sources of vibration. In order to simplify the problem, the SSI is not considered in this section, i.e. the wind turbine is fixed at ground level. In Figure 0 the displacements are shown for the two conditions analyzed. These results refer to the displacement of the tower to the two directions

considered in this work, out-of-plane and in-plane.

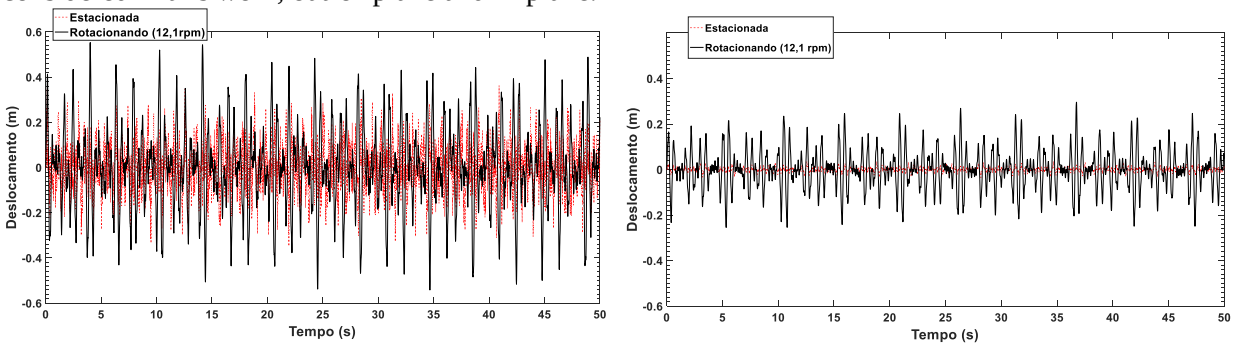


(a) *fora-do-plano* (b) *no-plano*

Figure 10: Time-history of the top tower.

It is true that the responses along the tower are different and the maximum responses occur at the top of the tower. By concision, only the maximal responses are discussed in the present study, for both the blades and the tower.

In the Figure 10, the red lines represent the results when the blades are in the parked condition and the black lines are the shifts when they are rotating. In this way, it can be seen that the displacements in the operating condition are greater than those in the parked condition in both directions. As can be seen in the Figure 10, the maximum displacement for out-of-plane offsets at the top of the tower is 0.571 m occurring at t = 34.9 s when the wind turbine is in operation. When the blades are parked, a maximum displacement of 0.365 m occurs at t = 41.5 s. The Figure 10.*b* shows the displacements in the in-plane direction, it can be seen that the maximum values of these displacements are 0.053 and 0.296m, when the wind turbine is in the parked and operating conditions respectively.

These results were actually expected since, when the blades are rotating, the wind loads acting on the blades are larger compared to the parked condition. Larger wind loads on blades result in more severe interaction between the tower and the blades and, therefore, higher tower responses. Thus, these data indicate that previous studies, assuming that wind turbines in the parked condition, may result in estimates of non-conservative structural responses, which in turn may lead to unsafe design of structural components.

Comparing the Figure 10.*a* and Figure 10.*b* it can be seen that the displacements in the 'in-plane' direction of the tower are much smaller than the 'out-of-plane' responses in both cases. Two reasons lead to these results. The first is that wind and earthquake loads are applied only in the out-of-plane direction of the tower in the present work, and no external source of vibration is driven in the 'in-plane' direction. The other reason is that the wind loads in the blades in the 'out-of-plane' and 'in-plane' directions are almost the same when the wind turbine is in the parked condition, while when in the operating condition, the wind loads in the direction away from the plane of rotation are much greater than those in the direction of the plane of rotation. The higher wind loads on the blades result in a more severe interaction between the tower and blades and lead to higher tower responses in the out-of-plane direction as discussed above. In addition, there is also the load due to the earthquake that also acts in the out-of-plane direction.

Figures 11 and 12 show the acceleration response PSDs at the top of the tower in the out-of-plane and in-plane directions, respectively, when the blades are in operating and parked conditions. As shown in Fig. 11, a clear peak appears at 0.34 Hz. As shown earlier this value corresponds to the tower's first vibration mode in the off-plane direction, meaning that the first vibration mode is excited by the external sources of vibration. Fig. 11 also shows that another peak occurs at 0.591 Hz and 0.583 Hz, respectively, when the wind turbine is in steady and operational conditions. As shown earlier, this is the first mode of blade vibration when wind turbine. These results again indicate that the interaction between the tower and the blades causes the vibrations of the blades to contribute to the tower responses. Compared to the parked condition, the first blade vibration frequency is slightly higher when in the operating condition, as shown in Fig. 11. This is because the centrifugal blade rigidity is

generated when the wind turbine is operating, which in turn leads to high structural rigidity and frequency of blade vibration.

For PSDs in the foreground direction, Fig. 12 shows that a peak appears at 0.312 Hz, and this peak corresponds to the tower's first vibration mode in the foreground direction. Comparing the results in Fig. 12 with those of Fig. 11, it is evident that the energies are much lower in the in-plane direction, which results in lower tower responses in this direction, as shown in Fig. 10. Similarly, compared to the black curve, the values on the red curve are larger, and this explains the larger structural responses in the operating condition, as shown in Figure 10.

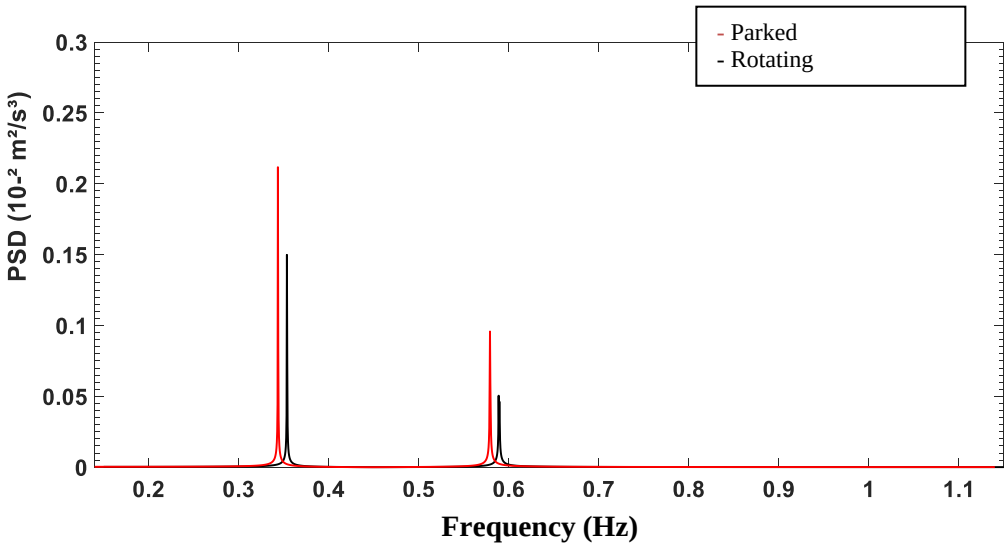


Figure 11: PSD of the top-of-tower acceleration response in the out-of-plane direction when the blades are in operating condition and parked.

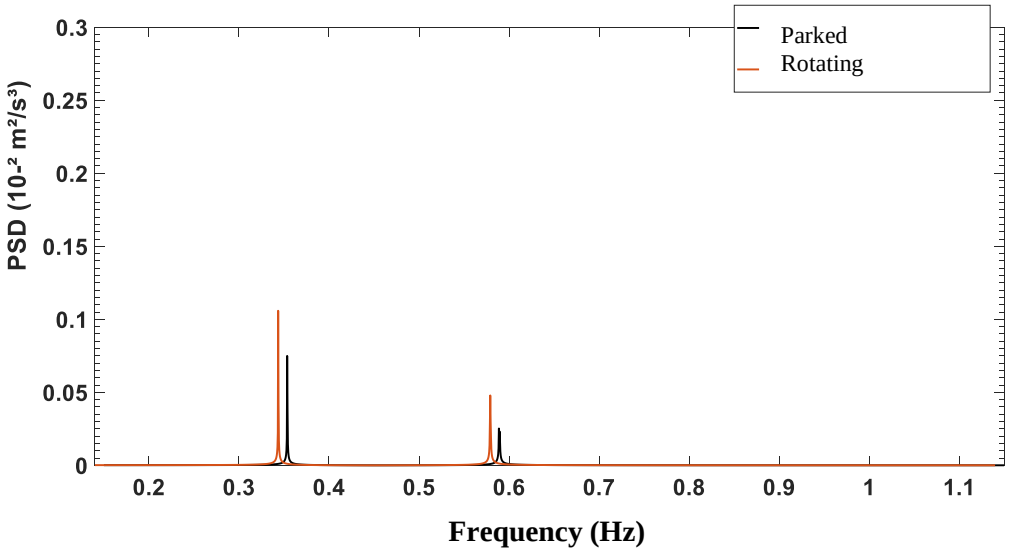


Figure 12: Tower top acceleration response PSD in the in-plane direction when the blades are in operating condition and parked.

Sequentially, the same operating conditions and their influences on blade responses were analyzed. The Figure 13 shows the displacement over time at the blade tips in the out-of-plane direction. The out-of-plane offsets at the blade tips 1, 2 and 3 are 0.509 m, 0.451 m and 0.404 m, respectively when the wind turbine is in the parked condition. The displacements at the blade tips are different. This is because the blade locations shown in Figure 13, are not the same, which generates different influences of the weight itself, and even if the applied excitations are the same the structural

responses are different. The result also shows that the maximum displacement in the out-of-plane direction in blade 3 is less than in blades 1 and 2, because the blade's own weight on blade 1 generates greater traction than those on Blades 2 and 3 and this contributed to increase the stiffness of the blade.

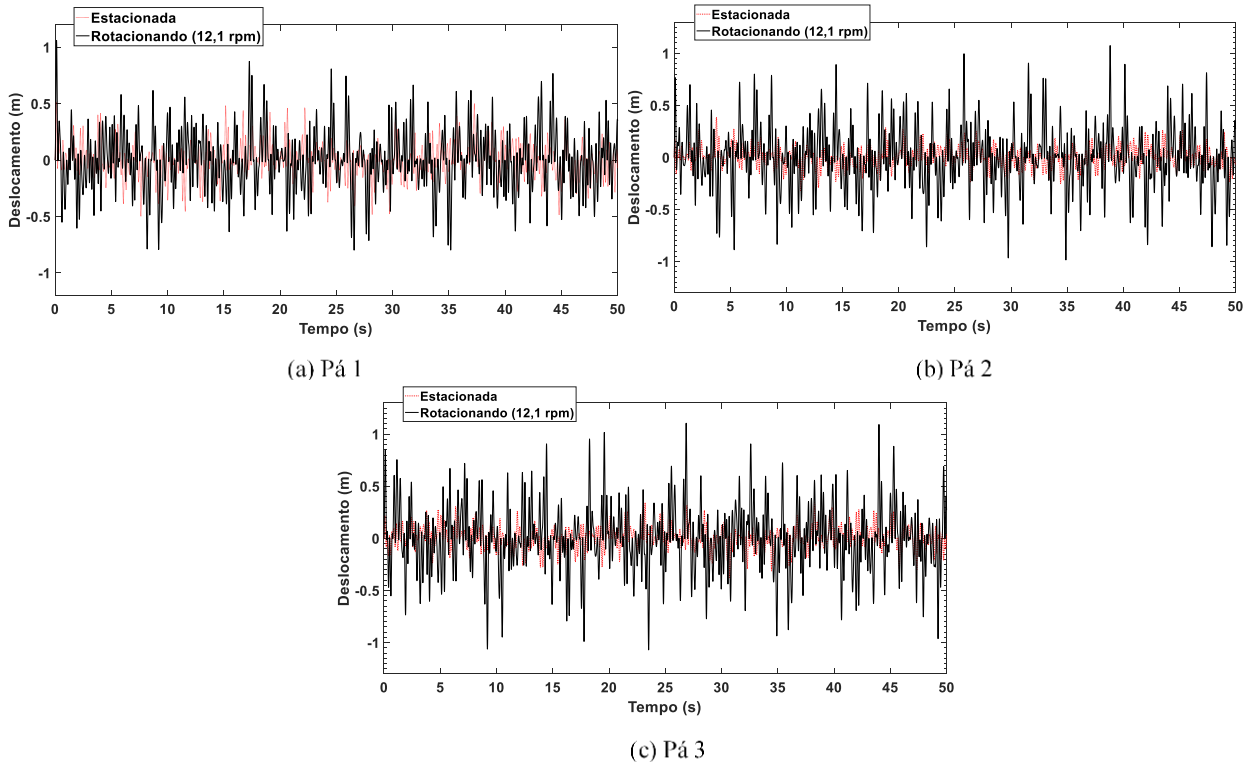


(a) Pá 1 (b) Pá 2

(c) Pá 3

Figure 13: Time-history of the Blades in the out-of-plane direction.

The Figure 13 also shows that the maximum displacements are much greater when the blades are rotating, and the corresponding values are 1,024 m, 1,102 m and 1,114 m respectively. This small difference is due to the fact that when the wind turbine is in the operating condition, the vibrations of the blades are not the same and are influenced by the locations where the blades originated when the rotation started.

The Figure 14 shows the blade tip displacements when they are in parked conditions and also in operation, in the direction out of the plane of rotation. As shown in the Figure 14, the maximum lateral edge displacements at the tips of Blades 1, 2 and 3 are 0.097 m, 0.108 m and 0.105 m, respectively, when the turbine is in the parked condition. The responses of the three blades are very similar because all three have the same geometrical and structural parameters in the rotor plane. When the blades are rotating, as shown in Figure 14, the response at the tips of Blades 1, 2 and 3 are 0.341 m, 0.325 m and 0.345 m, respectively. Compared to the parked condition, blade displacements are much larger when rotating, this is for the same reason as in the tower, explained previously.

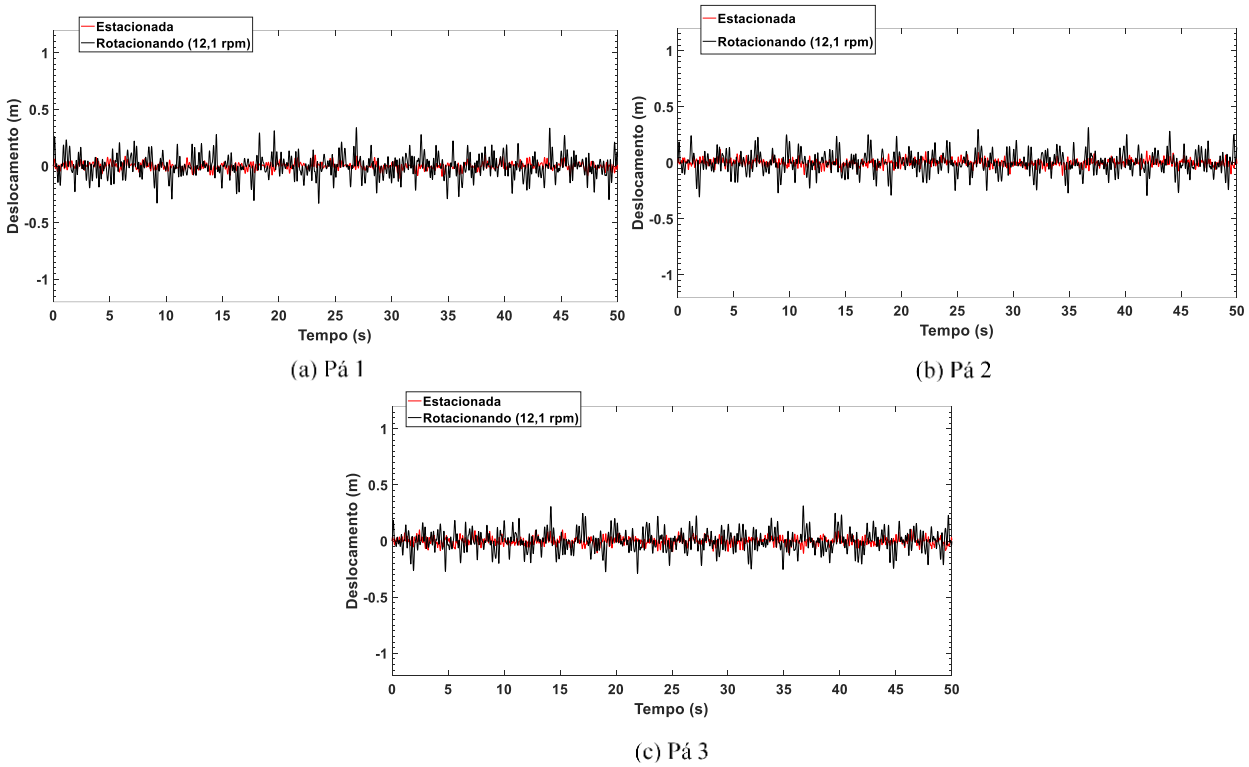


Figure 14: Time-history of the Blades in the in-plane direction.

### 5.3 Influence of the SSI

In order to investigate the effect of the SSI on dynamic wind turbine behavior, three different soils with shear strength are considered in the present study and are used to represent typical soft, medium and rigid soils (Table 3). The same excitation sources used previously are considered here.

As shown in Figure 15, the consideration of the SSI can significantly decrease the vibration frequencies of the tower especially for the soft soil condition. This is because the consideration of the foundation is surrounded by the soil and this undergoes displacements makes the tower more flexible, compared to the case of the wind turbine totally fixed in the soil and this does not deform (if the SSI is not considered). As the rigidity of the tower becomes smaller, the vibration frequencies of the tower therefore decrease. For example, when the shear strength is 25 kPa, the first vibration frequency of the tower in the out-of-plane direction is 0.28 Hz and is 0.33 Hz when the SSI is not considered. The rate of reduction is 15.2%. It should be noted that the energy of the wind load is concentrated within the range of 0 to 0.25 Hz [1], when the SSI is considered, the first vibration frequency of the tower is closer to the dominant frequency of the wind load . In this case, resonance may occur, and larger structural responses are expected. Therefore, the SSI should be considered to more accurately predict the dynamic responses of the wind turbine.

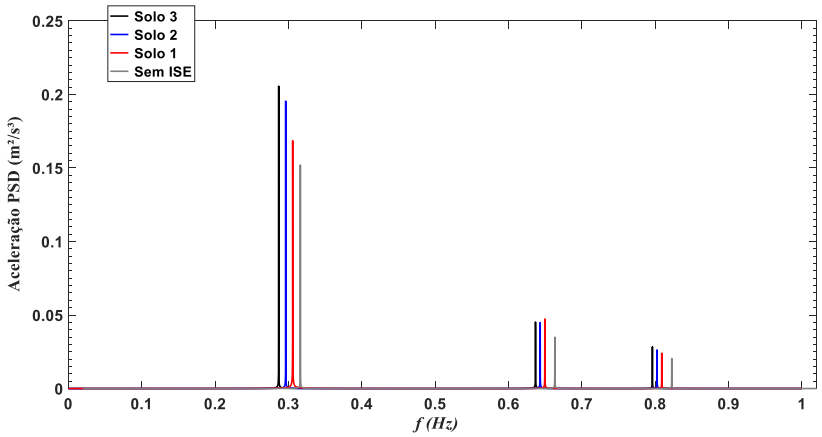


Figure 15: Tower frequencies for different soil conditions.

Unlike the modal analysis, the wind turbine is assumed in the operating condition when the structural responses are calculated. In this section, a rotor angular velocity of 12.1 rpm is considered. The Figure 15 shows the spectral power densities of the acceleration responses at the top of the tower in the out-of-plane directions without and with the SSI effect. As shown, the first vibration frequency of the tower in the out-of-plane direction shifts to a lower value when the SSI is considered, and they are 0.28 Hz, 0.293 Hz and 0.313 Hz when the foundation is embedded in Soil 1, Soil 2 and Soil 3 respectively. The Figure 15 also shows that the higher energy is obtained for the softer soil, which, in turn, results in higher tower responses, as shown in Figure 16.

The Figure 16 shows the displacement over time at the top of the tower in the out-of-plane direction without and with consideration of SSI. Table 5 shows the maximum out-of-plane offsets at the top of the tower, and the corresponding differences between the offsets with and without SSI are given in the table as well. As shown in Figure , tower vibrations are much larger in out-of-plane directions when SSI is considered, and with increased soil shear strength, the lateral stiffness of the soil increases and consequently there are decreases in deflection of the tower. The out-of-plane offsets at the top of the tower are 1.331 m, 1.223 m and 0.947 m when the foundation is embedded in soil 1, soil 2 and soil 3 respectively, which increases the responses in 101.2%, 85.2% and 43.5% compared to the value when the wind turbine is fixed in the soil (0.66 m), i.e. neglecting the interaction between the foundation and the surrounding soil (Figure 16).

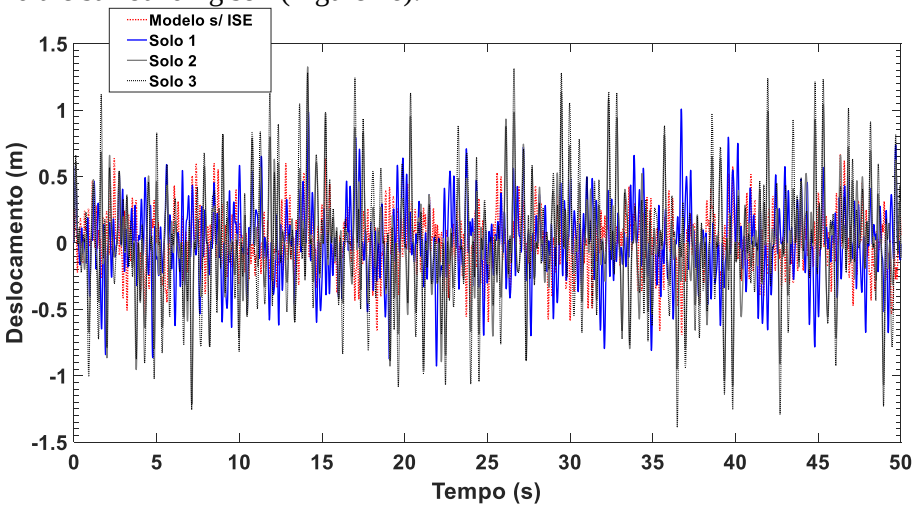


Figure 16: Time-history of the tower in the out-of-plane direction for different soil conditions.

For the displacement analysis of the blades, by simplification, only the blade responses were considered. The Figure 17 shows the displacements at the blade tips 1 over time out-of-plane. Table 5 shows the maximum displacement at the tip of blade 1 and the corresponding differences when the SSI is considered or not. It is verified that the greatest

displacements at the tip of Blade 1 are 1.606, 1.431 and 1.220 m when the foundation is embedded in soil 1, soil 2 and soil 3 respectively, which increases the responses in 59.0%, 41.7% and 20.9%, respectively, compared to the value when the wind turbine is fixed to the ground (1.01 m).

Table **Erro! Nenhum texto com o estilo especificado foi encontrado no documento.**: Maximum tower displacement considering the SSI.

| | **Without SSI (m)** | **Soil 1 Displacement (m)** | **Difference (%)** | **Soil 2 Displacement (m)** | **Difference (%)** | **Soil 3 Displacement (m)** | **Difference (%)** |
|---|---|---|---|---|---|---|---|
| **Tower** | 0,606 | 0,947 | 43,5 % | 1,223 | 85,2 % | 1,331 | 101,2 % |

It can be observed that the blade displacement responses are influenced by the SSI, but less significantly than the tower responses (Table 5). This is because the soil springs are directly connected to the foundation of the tower, while the influence of the SSI on the blades is mainly through the (indirect) interaction between the tower and the blades. As discussed above, the softer soil leads to greater front and side vibrations of the tower, which, in turn, leads to more severe interaction between the tower and the blades and, therefore, the greater blade displacements.

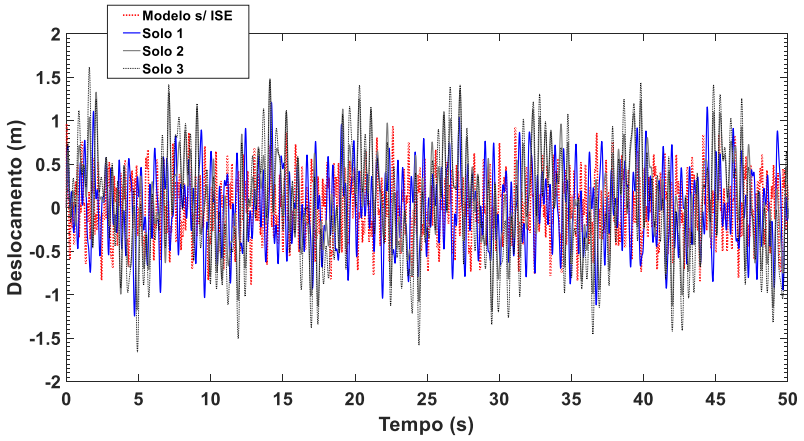


Figure 17: Displacement of the Blade 1 in the out-of-plane direction for different soil conditions.

The Figure 18 shows the lateral displacement at the tip of Blade 1 over time, and the displacements on the other two blades are not shown to be too close. As expected, again the rotational blade edge shifts are governed by rotor rotation, this implies that the SSI has an insignificant effect on blade displacement responses in the in-plane direction. It occurs for the reason that the vibrations of the tower in the lateral direction are very small, as shown in Figure 18Figure , which outcomes in unimportant interactions between the tower and the blades in this sense. The results are in good agreement with those reported by Fitzgerald and Basu [6].

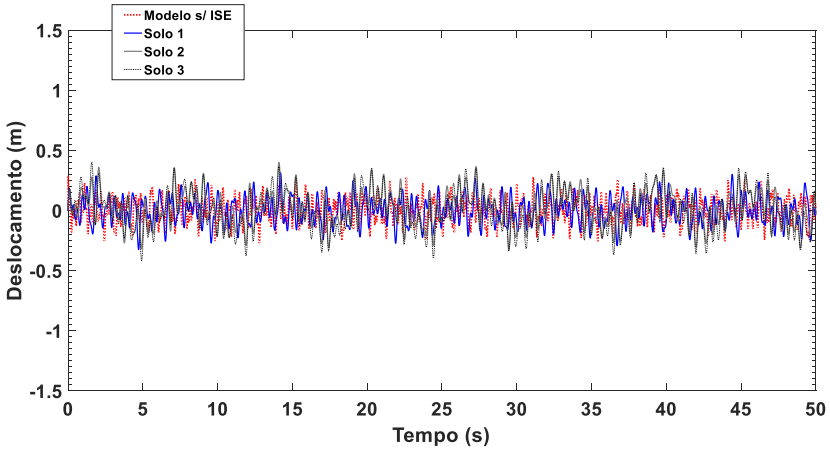


Figure 18: Displacement of the Blade 1 in the in-plane direction for different soil conditions.

Table 6: Maximum displacement of Blade 1 in both directions (in-plane and out-of-plane) considering SSI.

| Blade 1 | w/o SSI (m) | Soil 1 Displacement (m) | Soil 1 Difference (%) | Soil 2 Displacement (m) | Soil 2 Difference (%) | Soil 3 Displacement (m) | Soil 3 Difference (%) |
|---|---|---|---|---|---|---|---|
| **Out-of-plane** | 1,01 | 1,220 | 20,9 % | 1,431 | 41,7 % | 1,606 | 59 % |
| **In-plane** | 0,325 | 0,351 | 8,0 % | 0,388 | 19,4 % | 0,401 | 23,4 % |

## CONCLUSIONS

In general, this work investigated the dynamic behavior of wind turbines. subjected to wind and earthquake loading. For this, studies were carried out on the dynamic model responses of the NREL 5MW wind turbine. Influences of operating conditions, soil-structure interaction, and rotor speed on tower and blades are examined. Based on the results reported here, the following conclusions can be drawn:

The maximum displacements, due to wind and earthquake, at the top of the tower in the out-of-plane and in-plane directions when the wind turbine rotates with a rotor speed of 12.1 rpm are greater than those when the turbine is in condition parked The peak displacement of the blades in the direction of the plane of rotation is about ***5 times*** that of the wind turbine parked in the same direction. This is because when the blades are parked the loads in the out-of-plane direction are much smaller, in addition the blades have greater stiffness in the in-plane direction than in the out-of-plane direction. Thus, studies assuming that wind turbines are in the parked condition may result in estimates of non-conservative structural response generating an unsafe design of the structural components. In current design standards, safety factors are commonly used to explain uncertainties and variability in loads, methods of analysis and the importance of structural components for wind turbines. However, it would be interesting to develop a uniform safety factor that can be used to estimate operational response based on parked results; for this, however, more comprehensive research papers are needed.

The vibration frequencies of the tower are significantly reduced when the SSI is considered, however the same reduction magnitude is not verified in the responses and consequently in the natural frequency of the blades, in which the SSI has a smaller effect.

By analyzing the displacement responses of the tower and the blades, it is possible to see that the SSI influences substantially, increasing the displacement the more flexible the soil, in the out-of-plane direction. However, SSI does not have the same effect on blade displacements in the in-plane direction.

It should be noted that wind is not the dominant charge in the present study but the earthquake. In addition, all of the above findings are derived from the NREL 5MW wind turbine, which is one of the

largest wind turbines in the world today; therefore, they can only apply to this group. To apply the present results in engineering practice and to guide projects for all groups of wind turbines (i.e. including groups of small and medium wind turbines as well), more comprehensive analyzes are needed.

## References


[1] H. Zuo, K. Bi, and H. Hao, "Dynamic analyses of operating offshore wind turbines including soil-structure interaction," *Eng. Struct.*, vol. 157, no. June 2017, pp. 42–62, 2018.

[2] M. Harte, B. Basu, and S. R. K. Nielsen, "Dynamic analysis of wind turbines including soil-structure interaction," *Eng. Struct.*, vol. 45, pp. 509–518, 2012.

[3] D. Witcher, "Seismic analysis of wind turbines in the time domain," *Wind Energy*, vol. 8, no. 1, pp. 81–91, 2005.

[4] H. R. and E. D. Ian Prowell, Ahmed Elgamal, Chia-Ming Uang, J.Enrique Luco, "Shake table testing and numerical simulation of a utility-scale wind turbine including operational effects," *Wind Energy*, no. January, pp. 677–689, 2014.

[5] B. Fitzgerald and B. Basu, "Cable connected active tuned mass dampers for control of in-plane vibrations of wind turbine blades," *J. Sound Vib.*, vol. 333, no. 23, pp. 5980–6004, 2014.

[6] B. Fitzgerald and B. Basu, "Structural control of wind turbines with soil structure interaction included," *Eng. Struct.*, vol. 111, pp. 131–151, 2016.

[7] A. s. and B. V. VELETSOS, "VIBRATION OF VISCOELASTIC FOUNDATIONS," *Int. J. Rock Mech. Min. Sci. Geomech. Abstr.*, vol. 11, no. 8, p. A171, 1973.

[8] J. P. Stewart, "SOIL-STRUCTURE INTERACTION EFFECTS by Raymond B . Seed and Gregory L . Fenves Report No . PEER-98 / 07 Pacific Earthquake Engineering Research Center University of California Berkeley , California November 1998 ii," *Environ. Eng.*, no. November, 1998.

[9] D. Lombardi, S. Bhattacharya, and D. Muir Wood, "Dynamic soil-structure interaction of monopile supported wind turbines in cohesive soil," *Soil Dyn. Earthq. Eng.*, vol. 49, pp. 165–180, 2013.

[10] S. Bhattacharya and S. Adhikari, "Experimental validation of soil-structure interaction of offshore wind turbines," *Soil Dyn. Earthq. Eng.*, vol. 31, no. 5–6, pp. 805–816, 2011.

[11] S. Austin and S. Jerath, "Effect of soil-foundation-structure interaction on the seismic response of wind turbines," *Ain Shams Eng. J.*, vol. 8, no. 3, pp. 323–331, 2017.

[12] W. S. Kim, C. Jeoung, K. M. Lee, and J. H. Lee, "Seismic Analysis of Concrete Conical Foundation for 5 MWWind Turbine," *Adv. Mater. Res.*, vol. 831, pp. 133–136, 2013.

[13] W. Turbines and S. Edition, *Guidelinse for Design of Wind Turbines*. 2002.

[14] P. J. Murtagh, A. Ghosh, B. Basu, and B. M. Broderick, "Passive control of wind turbine vibrations including blade/tower interaction and rotationally sampled turbulence," *Wind Energy*, vol. 11, no. 4, pp. 305–317, 2008.

[15] A. Staino and B. Basu, "Dynamics and control of vibrations in wind turbines with variable rotor speed," *Eng. Struct.*, vol. 56, pp. 58–67, 2013.

[16] Z. Zhang, A. Staino, B. Basu, and S. R. K. Nielsen, "Performance evaluation of full-scale tuned liquid dampers (TLDs) for vibration control of large wind turbines using real-time hybrid testing," *Eng. Struct.*, vol. 126, pp. 417–431, 2016.

[17] H. Zuo, K. Bi, and H. Hao, "Influence of Soil-Structure Interaction on the Dynamic Behaviours of Offshore Wind Turbi ....," no. February, 2018.

[18] R. W. Clough and J. Penzien, *Dynamics of Structures*. 2013.

[19] M. O. L. Hansen, *Aerodynamics of Wind Turbines*, vol. 130, no. 9. 2015.

[20] M. H. Hansen, "Improved modal dynamics of wind turbines to avoid stall-induced vibrations," *Wind Energy*, vol. 6, no. 2, pp. 179–195, 2003.

[21] H. Hu, Z. Yang, and P. Sarkar, "Dynamic wind loads and wake characteristics of a wind turbine model in an atmospheric boundary layer wind," *Exp. Fluids*, vol. 52, no. 5, pp. 1277–1294, 2012.

[22] W. Wang and B. Wang, "Model Test and Numerical Analysis of an Offshore Bottom Fixed Pentapod Wind Turbine under Seismic Loads," pp. 1–11, 2017.

[23] A. Elmi, "Time-Domain Dynamic Response of Operational Wind Turbines Considering Soil-Structure Interaction," no. October, 2017.

[24] F. Khosravikia, M. Mahsuli, and M. A. Ghannad, "Comparative Assessment of Soil-Structure Interaction Regulations of ASCE 7-16 and ASCE 7-10," no. January, pp. 388–399, 2018.

[25] NEHRP Consultants Joint Venture, "Soil-Structure Interaction for Building Structures," *Nist Gcr*, vol. 12, pp. 917–21, 2012.

[26] R. A. Kjørlaug, A. M. Kaynia, and A. Elgamal, "Seismic Response of Wind Turbines due to Earthquake and Wind Loading," *EURODYN 9th Int. Conf. Struct. Dyn.*, no. July, pp. 3627–3634, 2014.

[27] P. E. M. Al Satari and S. E. S. Hussain, "Vibration Based Wind Turbine Tower Foundation Design Utilizing Soil-Foundation-Structure Interaction," *AIP Conf. Proc.*, vol. 1020, no. 1, pp. 577–584, 2008.

[28] M. Alhamaydeh and S. Hussain, "Optimized frequency-based foundation design for wind turbine towers utilizing soilstructure interaction," *J. Franklin Inst.*, vol. 348, no. 7, pp. 1470–1487, 2011.